A Novel Equivalence Principle for Quantum Gravity

Hans-Otto Carmesin*

*Studienseminar Stade, Bahnhofstraße 5, 21682 Stade, Athenaeum Stade, Harsefelder Straße 40, 21680 Stade,
University Bremen, Otto – Hahn – Alle 1, 28359 Bremen
Hans-Otto.Carmesin@athenetz.de

Abstract

The evolution of the early universe is a challenging topic for students in research clubs or similar learning groups. Here we study sub curvature length scales. For these small lengths a novel equivalence principle becomes valid. This principle can be successfully applied to the cosmic inflation, dark energy and dark matter. The first two applications are worked out in full detail here so that they can be directly used in a learning group.

1. Introduction

The universe has always been interesting to humans (Hoskin 1999). Accordingly students like to take part in astronomy clubs or they choose astrophysical projects in a research club. These interests provide chances for scientific education. Here I outline a corresponding project, and I report about experiences with teaching it.

1.1. Early universe: a lab for quantum gravity

In the early universe, the density was very high, and so gravity was the dominating interaction. Moreover, distances were very small, and so quantum physics is essential. Additionally, there are many corresponding observations. So the early universe is an ideal lab for the combination (Bronstein 1936) of gravity and quantum physics.

1.2. Challenging questions

In the early universe, there occurred a very rapid increase of distances in the so-called era of cosmic inflation (Guth 1981), the dark matter (Zwicky 1933) formed, and the dark energy emerged (Einstein 1917; Perlmutter et al. 1998; Riess et al. 2000; Smoot 2007). The explanation of these phenomena is possible in the framework of quantum gravity (Carmesin 2017, Carmesin 2018a-d, Carmesin 2019). So this is an interesting actual topic for a research club.

1.3. Analogies

In order to obtain a smooth learning process, we introduce and investigate the concepts of the harmonic oscillator and of the waves in crystals. Progressively we develop novel concepts by using analogies to these basic two concepts. Additionally we use the Heisenberg uncertainty relation, the Schwarzschild radius and the Friedmann Lemaitre equation, FLE, as basic concepts (Carmesin 2014).

2. Students

The present project has been tested in a research club with students in classes 9 to 12. The students also attend an astronomy club and apply computers.

3. Observable States

Physical states can only be observed, if the Heisenberg uncertainty relation is fulfilled (Heisenberg, 1927):

$$\Delta x \cdot \Delta p \geq ½ \cdot \underline{h} \qquad \{1\}$$

Hereby $\underline{h}$ denotes the reduced Planck constant $h/2\pi$, x the coordinate and p the momentum. Furthermore, only a spatial physical structure r outside the Schwarzschild radius R_S can be observed (Michell 1784; Schwarzschild, 1916):

$$r \geq R_S = 2 \cdot G \cdot m/c^2 \qquad \{2\}$$

Hereby G denotes the gravitational constant, m the mass and c the velocity of light. Consequently, only states in the dark shaded area in figure (1) can be observed.

Accordingly, we introduce the concept of a region without observable internal spatial structure. Such a region is called elementary region ER. There are two ERs at a fixed density (see figure 1): Each mass m is surrounded by a ball with radius R_S, and this ball is an ER (see upper triangle in figure 1, we denote that radius by b). For each point in space, we derive the best spatial resolution. Best resolution is achieved according to the uncertainty relation (equation 1) with the equality sign and with relativistic radiation with $\Delta p = E/c$. We express this equation in Planck units (Planck 1899). So we get:

$$\mathbf{\Delta x} = 1/(2 \cdot \mathbf{E}) \qquad \{3\}$$

In Planck units, the energy **E** is equal to the corresponding mass **M**. Accordingly, we denote the above uncertainty by a_M:

$$2 \cdot \mathbf{a_M} = 1/\mathbf{E} = 1/\mathbf{M} \qquad \{4\}$$

The ball with that radius $\mathbf{a_M}$ is the other ER at the considered fixed density, see full triangle in figure 1. When the density increases, then the two elementary regions, the b – ER and the a_M – ER approach each other in figure (1), and they merge at the smallest possible ER (see full circle in figure 1). Hereby the radius is the Planck length L_P, the energy is half the Planck energy E_P , the ρ density is half the Planck density ρ_P , and that density ρ is the highest achievable density (see Carmesin 2017, 2018a-d, 2019).

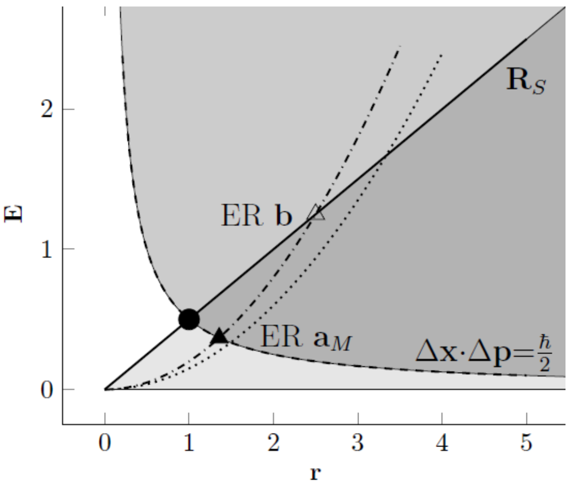

Fig.1: Planck Scale: Planck units: bold face. Distance: **r**. Energy: **E**. Circle: Planck length L_P. Triangles: elementary regions ER. Light shaded: observable according to uncertainty relation. Medium shaded: observable according to Schwarzschild radius R_S. Dark shaded: observable. Dash-dotted: fixed density. Dotted: lower fixed density.

4. Model

In order to combine gravity and quantum physics, it is essential to determine the microscopic objects that should be described. It is natural to model the ERs microscopically. This is worked out next.

5. Microscopic part of the model

We model a **b** – ER and a neighboring $\mathbf{a_M}$ – ER in a microscopic part of the model. Next we investigate the properties of that model.

5.1. Isotropy

These two ERs are at a distance $\mathbf{a} = \mathbf{a_M} + \mathbf{b}$. That distance is characterized by a wave function. Since gravity is very large, everything tends 'to fall down', and so we model ground states here. Correspondingly, we model that distance with an isotropic wave function.

5.2. Dynamics

According to the isotropy, we apply an isotropic version of general relativity. The corresponding cosmological dynamics is described by the Friedmann Lemaitre equation, FLE (Friedmann 1922, Lemaitre 1927):

$$[a'(t)/a(t)]^2 = 8\pi G\cdot\rho/3 - k\cdot c^2/a^2 \qquad \{5\}$$

Hereby, k describes the curvature of the isotropic space, and it is called the curvature parameter.

5.3. Mathematical equivalence

The students can easily derive that the FLE is mathematically equivalent to the following equation:

$$E = ½ \cdot m \cdot v^2 - G\cdot M\cdot m/a \qquad \{6\}$$

Thereby, M describes the equivalent mass of the a_M - ER, m denotes the mass of the b – ER, v describes $a'(t)$, and E describes the curvature parameter as follows:

$$E = -m\cdot c^2\cdot k/2 \qquad \{7\}$$

5.4. Novel equivalence principle

The FLE describes curved space in general. However, the mathematically equivalent equation {6} does not include the curvature parameter explicitly. Accordingly, we investigate the possible physical equivalence. Thereby, we call two systems physically equivalent, if no difference can be observed. In a system consisting of two neighboring ERs, no curvature can be observed geometrically, since the curvature can only be observed with at least three ERs (Lee 1997). This corresponds to the fact that two points determine a straight line, whereas three points determine a radius of curvature. As a consequence, the curvature parameter cannot be observed geometrically in the microscopic part of the system. Consequently, the FLE and the dynamics of equation {6} are mathematically and physically equivalent at the small length scale of the microscopic part of the model.

5.5. Analogy

The microscopic part of the model includes the phenomenon of the curvature of space, though it is not included explicitly in equation {6}. Similarly, the motion of molecules in a gas may be described by Newtonian mechanics without an explicit force of friction, and as a result, that description provides an effective force of friction (see for instance Carmesin 2019).

5.6. Quantization

The dynamic equation {6} is quantized by the usual rules of quantum physics (see Schrödinger 1926 or for instance Ballentine 1998). Accordingly, the observable quantities are replaced by operators. Thereby the observable quantities in equation {6} are the coordinate a with the corresponding momentum $p = m\cdot a'(t)$, and the variable E is identified with the energy according to the form of equation {6}. The Schrödinger equation with the operator of E describes the dynamics. That quantization is uniquely determined, as there occur no products with different operators.

5.7. First method of investigation

First we investigate solutions of the stationary Schrödinger equation. In particular we determine ground states first. Hereby we consider the limit of high density and small distances first. In that limit, the wave functions are Gaussian wave packets and the expectation value of the potential energy is a harmonic potential (see Carmesin 2019). In order to obtain a low barrier of learning, we determine expectation values. So we investigate the harmonic oscillator first.

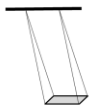

Fig.2: A swing is an example for a harmonic oscillator.

6. Ground state of harmonic oscillator

First we investigate the harmonic oscillator, as it is essential here, and as it is interesting by itself (see figure 2). The students formulate the energy term:

$$E = p^2/(2m) + ½\ \kappa \cdot x^2 \qquad \{8\}$$

Hereby, κ denotes Hooke's constant.

6.1. Derivation of ground state

We apply the expectation values:

$$< E > = < p^2 >/(2m) + ½\ \kappa \cdot < x^2 > \qquad \{9\}$$

Here the students easily apply the mathematical identity

$$< x^2 > = < x >^2 + (\Delta x)^2, \qquad \{10\}$$

whereby the square of the uncertainty $(\Delta x)^2$ denotes $< (x - < x >)^2 >$. So they get:

$$< E > = < p >^2 /(2m) + ½\,\kappa \cdot < x >^2 + E_Q \qquad \{11\}$$

Hereby E_Q is the additional quantum term:

$$E_Q = (\Delta p)^2 /(2m) + ½\,\kappa \cdot (\Delta x)^2 \qquad \{12\}$$

For Gaussian wave functions, the students verify with help of a working sheet that the uncertainty relation achieves the minimal uncertainty:

$$\Delta x \cdot \Delta p = ½ \cdot \underline{h} \qquad \{13\}$$

With it they derive (see equation {12}):

$$E_Q = \underline{h}^2 /[8m(\Delta x)^2] + ½\,\kappa \cdot (\Delta x)^2 \qquad \{14\}$$

Here the students determine the quantum fluctuations $q = (\Delta x)^2$ by application of the variational method. So they derive the value of q that minimizes the above term for the quantum energy E_Q. So they get:

$$(\Delta x)^2 = q = \underline{h} /[4m\,\kappa]^{0,5} \qquad \{15\}$$

They insert this term into the above term for E_Q. So they obtain the ground state energy of the harmonic oscillator:

$$E_Q = ½ \cdot \underline{h} \cdot \omega \qquad \{16\}$$

Thereby ω denotes the familiar angular frequency:

$$\omega = [\kappa/m]^{0.5} \qquad \{17\}$$

While the classical ground state energy is zero, the quantum energy is nonzero (equation {16}). Such a nonzero ground state energy is called zero-point energy, ZPE, and its oscillation is called zero-point oscillation, ZPO (see equation {15}). Our result is in full accordance with quantum theory (Ballentine 1998). But can ZPOs be observed?

6.2. ZPO observed in a crystal

An atom in a crystal is at the minimum of the potential. That minimum can be locally approximated by a quadratic function of the coordinate (Fornasini and Grisenti 2015). So it represents a harmonic oscillator, and it should exhibit the quantum fluctuations $(\Delta x)^2$ of the ZPO presented in equation {15}. In fact, this can be observed (see figure 3).

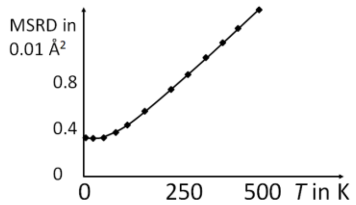

Fig.3: ZPO in a Cu crystal: The mean square relative displacement MSRD corresponds to the squared uncertainty. It is a function of the absolute temperature T (sketch on the basis of Fornasini and Grisenti 2015). The MSRD at zero K represents the ZPO. Diamonds: experiment.

6.3. Oscillators in crystals are coupled

The above oscillators in a crystal are coupled. This can be modeled by a partner swing (see figure 4). A partner swing exhibits two stable collective oscillations: the two oscillators can swing with the same phase and low frequency or with opposite phase and high frequency. If more swings are coupled, then these swings can form waves that oscillate at specific angular frequencies ω and corresponding energies $\underline{h}\omega$. The analogous waves in crystals are called phonons. Can these phonons be observed?

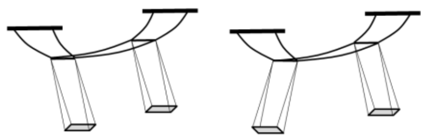

Fig.4: A partner swing: The oscillators oscillate in phase at the left and with opposite phase at the right.

6.4. Phonons observed in crystals

In a rhodium crystal, different phonons have been observed (see figure 5). Thereby, the phonons are marked on the horizontal axis, and the corresponding ZPEs are shown at the vertical axis. The theoretical calculations are presented by the lines and the corresponding measurements are presented by diamonds. The figure shows precise accordance of the modeled and observed ZPEs. This clearly confirms the concept of the ZPOs and ZPEs of waves.

Of course, there are also excited states corresponding to the ground states shown in figure (5).

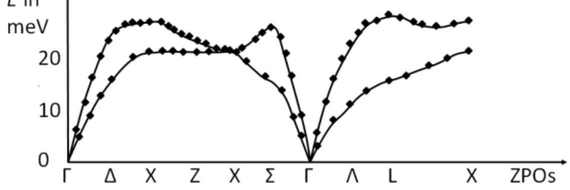

Fig.5: ZPEs of waves, so-called phonons, in a rhodium crystal (sketch on the basis of Heid, Bohnen and Reichardt 1999). Line: theory. Diamonds: measurement. Horizontal axis: phonons with typical notation of solid state physics. Vertical axis: ZPE in milli-eV.

7. Ground state of microscopic part

Next we apply the methods that we used for the harmonic oscillator. So we analyze the microscopic part of the model. Accordingly we get:

$< E > = < p^2 >/(2m) - G \cdot M \cdot m \cdot < a^{-1} >$ {18}

Here we apply the identity $a^{-1} = (a^2)^{-0.5}$. Furthermore we use the approximation $< (a^2)^{-0.5} > \approx (< a^2 >)^{-0.5}$.

And again we utilize equation {10}. So we get:

$$< E > = < p >^2 / (2m) + (\Delta p)^2 /(2m)$$
$$- G \cdot M \cdot m \cdot (< a >^2 + (\Delta a)^2)^{-0.5}$$

Here we expand in linear order in $(\Delta a)^2/< a >^2$. So we obtain:

$< E > = < p >^2 /(2m) + E_{cl,G} + E_Q$ {19}

Hereby $E_{cl,G}$ is the non-quantum gravity term

$E_{cl,G} = - G \cdot M \cdot m/< a >$ {20}

and E_Q is the additional quantum term:

$E_Q = (\Delta p)^2/(2m) + ½\, G \cdot M \cdot m \cdot (\Delta a)^2/< a >^3$ {21}

Again we use equation {13}. So we get:

$E_Q = \underline{h}^2/[8m \cdot (\Delta a)^2] + ½\, G \cdot M \cdot m \cdot (\Delta a)^2/< a >^3$ {22}

7.1. Higher dimension

At high density, gravity is very strong and tends to make objects very compact. Examples are white dwarfs, neutron stars and black holes. Another example for a very compact object is a parachute: in the unfolded state it is practically two dimensional and large, while in the folded state it is three dimensional and small. This example shows that compact objects can be generated by an increase of the dimension. Have dimensions larger than three been observed experimentally? Yes, four dimensional states have been observed in two different experiments that realize the four – dimensional quantum Hall effect (Lohse et al. 2018; Zilberberg 2018 et al.). Accordingly, we generalize our model to dimensions $D \geq 3$. For it, the potential energy term

$E_{pot} = - G \cdot M \cdot m / < a >$ {23}

is replaced by the following term:

$E_{pot} = - G \cdot L_P^{D-3} \cdot M \cdot m / < a^{D-2} >$ {24}

The exponent $D - 2$ is a consequence of Gaussian gravity (Gauss 1813; Bures 2011), and the factor L_P^{D-3} can be derived by using the concept of the Schwarzschild radius (see Carmesin 2017, Carmesin 2019). With it we generalize equation {20}:

$E_{D,cl,G} = - G \cdot L_P^{D-3} \cdot M \cdot m/ < a >^{D-2}$ {25}

Here and in the following, we mark the dependence of the energy on D by a subscript. In D dimensional isotropic space, the uncertainty relation {13} becomes:

$\Delta x \cdot \Delta p = ½ \cdot D \cdot \underline{h}$ {26}

So the quantum term is generalized as follows:

$$E_{D,Q} = D^2\underline{h}^2/[8m \cdot (\Delta a)^2]$$
$$+ ½ \cdot (D - 2) \cdot G \cdot L_P^{D-3} \cdot M \cdot m \cdot (\Delta a)^2/< a >^D \quad \{27\}$$

7.2. Planck units

In order to simplify the above equations, we use Planck units, we use the normalized energy E = $E/(m \cdot c^2)$, and we apply equation {4}. So we get:

$\underline{E}_{D,cl,G} = - 1/(2 \cdot < \mathbf{a_M} > \cdot < \mathbf{a} >^{D-2})$ {28}

Similarly we obtain:

$$\underline{E}_{D,Q} = D^2/[8\mathbf{m}^2 \cdot (\Delta \mathbf{a})^2]$$
$$+ (D - 2) \cdot (\Delta \mathbf{a})^2/(4 \cdot < \mathbf{a_M} > \cdot < \mathbf{a} >^D) \quad \{29\}$$

7.3. Quantum fluctuations

Here we investigate the case in which small particles have not yet formed. Then the distance **a** is approximately equal to **b**. Again the students determine the quantum fluctuations $q = (\Delta \mathbf{b})^2$ by application of the variational method. So they derive the value of q that minimizes the above term for the quantum energy $\underline{E}_{D,Q}$. So they get:

$(\Delta \mathbf{b})^4 = D^2 \cdot < \mathbf{a_M} > \cdot < \mathbf{b} >^D /[2(D - 2) \cdot \mathbf{m}^2]$ {30}

They insert this term into the above term for E_Q. So they obtain the ground state quantum energy:

$\underline{E}_{D,Q} = D \cdot [(D - 2) / [8 \cdot < \mathbf{a_M} > \cdot \mathbf{m}^2 \cdot < \mathbf{b} >^D]^{1/2}$ {31}

7.4. Density

Next we express the above two energies in terms of the density ρ_D in D dimensions. In isotropic Planck units (here the volume of a ball or hyperball is used, see Carmesin 2018a-d), the volume of a ball with a radius **b** is $\mathbf{V} = \mathbf{b}^D$, and the density is the mass per volume:

$\boldsymbol{\rho}_\mathbf{D} = \mathbf{m}/\mathbf{b}^D$ {32}

The Schwarzschild radius **b** can be derived according to the concept of Michell (see Michell 1784). So one gets (Carmesin 2017, Carmesin 2019):

$\mathbf{b} = (2 \cdot \boldsymbol{\rho}_\mathbf{D})^{-0.5}$ {33}

According to equations {4} and {32}, we derive the radius $\mathbf{a_M}$ as a function of $\boldsymbol{\rho}_\mathbf{D}$. So we get:

$< \mathbf{a_M} > = (2 \cdot \boldsymbol{\rho}_\mathbf{D})^{-1/(D+1)}$ {33}

We express $\underline{E}_Q$ (see equation {31}) in terms of ρ_D by using the above three relations. So we get:

$$\underline{E}_{D,Q} = \boldsymbol{\rho}_\mathbf{D}^{(3D \cdot D - D - 2)/(4D+4)}$$
$$\cdot 2^{(3D \cdot D - 3D - 4)/(4D+4)} \cdot D \cdot (D - 2)^{1/2} \quad \{34\}$$

Analogously we derive the classical gravity term (see equation {28}). So we obtain:

$$\underline{E}_{D,cl,G} = - \boldsymbol{\rho}_\mathbf{D}^{(D \cdot D - D)/(2D+2)}$$
$$\cdot 2^{(D \cdot D - 3D - 2)/(2D+2)} \quad \{35\}$$

7.5. Adiabatic separation

The term $< p >^2 /(2m)$ in equation {19} describes the term $a'(t)^2$. So it is the basis for the quantum physical generalization of the dynamics of the FLE (see Carmesin 2017, Carmesin 2018a-d). The other two terms in equation {19} characterize the faster dynamics of the formation of the wave function. We call the sum of these the reduced normalized energy $\underline{E}_{D,loc}$. So we get:

$\underline{E}_{D,loc} = \underline{E}_{D,Q} + \underline{E}_{D,cl,G}$ {36}

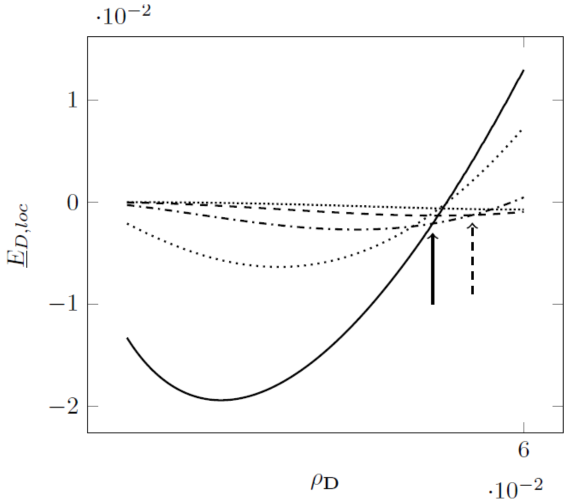

Fig.6: Energy $E_{D,loc}$ as a function of the scaled density ρ_D for dimensions 3 (solid line), 4 (dotted), 5 (dashdotted), 6 (dashed) and 7 (densely dotted). Arrows: dimensional transitions at critical densities $\rho_{D,c}$.

8. Dimensional transitions

According to the variational method, the energy E_D (see equations {34} – {36}) is minimized by variation of the dimension *D*. The students achieve this graphically (see figure 6) and numerically (Sprenger 2018). As a result, three dimensional space is stable at densities below $\rho_{D=3,c}$ = 0.0476. In the course of the expansion of the universe, the density decreased according to the FLE. Accordingly, when that density was reached, then there occurred a transition from five dimensional to three dimensional space. Similarly, five dimensional space formed from six dimensional space at the critical density $\rho_{D=5,c}$ = 0.053.

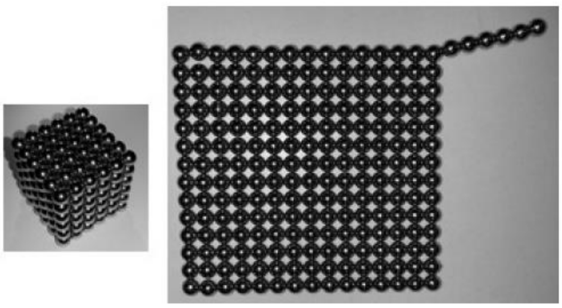

Fig.7: Enlargement illustrated by an analogy: Each magnetic ball corresponds to an ER. A dimensional transition from *D* = 3 to *D* = 2 is modeled. Note, the smallest possible dimension achieved by the present model is 3 (see Carmesin 2018a-d, Carmesin 2019).

9. Enlargement

At a dimensional transition from a higher dimension *D*+s to a lower dimension *D*, the space is enlarged by a factor $Z_{D+s\to D}$. This factor is derived by using a cubic or hypercubic model (see figure 7). At dimension *D+s*, there are *n* balls at an edge. Here we use the diameter as the unit. So we obtain the length L_{D+s} of that edge:

$$L_{D+s} = n \qquad \{37\}$$

By definition we get:

$$L_D = n \cdot Z_{D+s\to D} \qquad \{38\}$$

At the transition, the number of balls is invariant. So we obtain:

$$L_D^{\,D} = (n \cdot Z_{D+s\to D})^D = n^{D+s} \qquad \{39\}$$

We solve for $Z_{D+s\to D}$. So we get:

$$Z_{D+s\to D} = n^{s/D} \qquad \{40\}$$

10. Dimensional horizon

The space enclosed by the actual light horizon r_{lh} was smaller at earlier times according to the FLE. At the density $\rho_{D=3,c}$ = 0.0476, the corresponding volume consisted of 2^{301} ERs. If we analyze the dynamics backwards in time, then we realize that these ERs were folded to higher dimensions, and ultimately there were two ERs in each dimensional direction at the dimension 301. This dimension is called the dimensional horizon D_{max}. So we get:

$$D_{max} = 301 \qquad \{41\}$$

11. Time evolution

The whole time evolution from the dimensional horizon until today can be calculated. For it we derived the dynamics at the transition by using Fermi's golden rule (Carmesin 2018a-d, Carmesin 2019). The elaboration of this is not in the scope of the present report. However, we summarize the results of that time evolution here. The evolution of the radius is shown in figure (5). That time evolution is based on three numerical inputs only (see Carmesin 2017, Carmesin 2018a-d, Carmesin 2019): the three universal constants *G*, *c* and *h*. Moreover, that time evolution solves problems of the cosmic inflation: horizon problem, flatness problem, reheating problem, fine-tuning problem (see Carmesin 2017, Carmesin 2018a-d, Carmesin 2019).

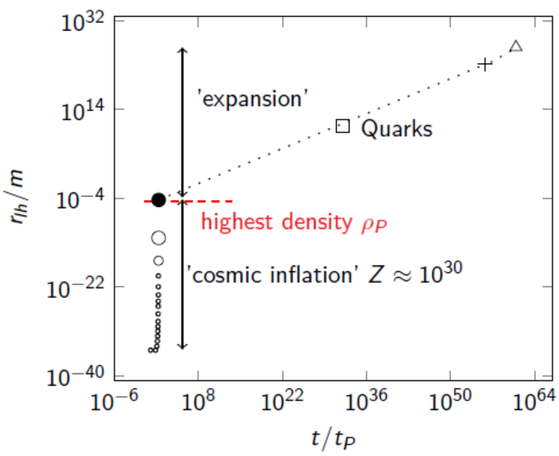

Fig.8: Time evolution of the actual light horizon (see Carmesin 2018a-d, Carmesin 2019): Triangle: today. Cross: density of radiation was equal to density of matter. Square: first quarks formed. Full circle: three dimensional space formed. Other circles: other dimensional transitions. Derived enlargement factor is in accordance to observations (Guth 1981; Broy 2016).

12. Model of the vacuum

The vacuum has a density (Einstein 1917; Perlmutter et al. 1998; Riess et al. 2000; Smoot 2007). This is modeled in this section. The model has been introduced in three different manners earlier (see Carmesin 2018a-d, Carmesin 2019). Here we introduce the model by developing an analogy to the phonons. Additionally we work out limitations of that analogy.

12.1. Waves

The density ρ_v of the vacuum is a property of space, properties of space are dominated by gravity (see Einstein 1915), and gravity should be generated by quantized gravitational waves in a quantum field theory. Also a phonon is a quantized wave. So there is an analogy.

12.2. Ground state

The density ρ_v of the vacuum exists even without any additional excitation. So ρ_v should be the density of a ZPO of a gravitational wave. Analogously, the phonons in figure (5) are ZPOs of waves.

12.3. Microscopic objects

The atoms exist together with the phonons, and the atoms are the basic oscillators that form the waves. Analogously, the ERs form microscopic objects that exist together with the quantized gravitational waves. Thereby the ERs are the basis of the space dimensions at which the waves form.

12.4. Boundary

Each phonon is within the boundaries of its crystal, and these boundaries determine the longest wave length of the phonons. Analogously, the quantized gravitational waves, that can have any influence upon us, are within the light horizon r_{lh}, and the longest wave length is determined by r_{lh}. There is a difference here: there are waves and wavelengths even beyond the light horizon.

12.5. Surrounding versus evolving structure

The phonon exists in a stable crystal, and the crystal exists in a stable space. Both structures have formed before the phonon can form. In particular, the oscillators of the phonon form in the potential that is formed by the crystal. Altogether a phonon forms in a structure that has formed before.

In contrast, the density ρ_v of the vacuum forms the space. There are only two structures in which the ZPO can form: The dimension D is formed according to the dimensional transitions based on the density of the ERs, and the light horizon is the boundary of causal influence upon us. So ρ_v is based on ZPOs that evolve in the course of time. These ZPOs are called evolving ZPOs, EZPOs.

12.6. Origin of EZPOs within light horizon

The EZPOs within the light horizon formed at the time of the dimensional horizon, as the earliest observable waves formed at that time. At D_{max}, the scaled density was $\boldsymbol{\rho_D} \approx ½$ in a very good approximation (see figure 1). Here we use this approximation, for more precise calculations see (Carmesin 2018b-c, Carmesin 2019). Correspondingly, the energy of a single mode was:

$$\mathbf{E_v}\,(D_{max}) = ½ \qquad \{42\}$$

Moreover, the scaled length of that mode was:

$$\mathbf{L}\,(D_{max}) = 1; \quad \mathbf{V} = \mathbf{L^D} = 1 \qquad \{43\}$$

At each dimension D, gravitational waves exhibit D modes of directions of propagation and $n_p = D - 1$ modes of transverse polarization. However, the maximal possible scaled density is ½, and at the scaled length $\mathbf{L} = 1$, the scaled density cannot be smaller than ½ (see figure 1). So the scaled density is ½. Correspondingly, this density is an average or linear combination of the single modes, and the averaged density is ½:

$$< \boldsymbol{\rho_v} > (D_{max}) = ½; \;\; n_p = D - 1 \qquad \{44\}$$

12.7. Relativistic EZPOs

The EZPOs are fully relativistic. So they propagate at the velocity of light. Accordingly, many EZPOs propagate through the length $\mathbf{L} = 1$ at D_{max}. Correspondingly, the occupation number of the EZPOs need not be one like in the case of phonons. Instead the occupation number of the EZPO is determined by the time evolution starting at D_{max}.

12.8. EZPOs at a dimensional transition

At a dimensional transition from dimension D+s to a dimension D, the length is enlarged by the factor $Z_{D+s \to D}$:

$$\mathbf{L}\,(D) = \mathbf{L}\,(D+s) \cdot Z_{D+s \to D} \qquad \{45\}$$

This enlarged length is available for the EZPOs, so the wavelength increases by that factor. Analogously, the longest wavelength of the phonons in a crystal increases by a factor Z, if the size of the crystal increases by that factor. So the EZPO experiences a redshift, and its ZPE decreases correspondingly. So the energy of a single mode is as follows:

$$\mathbf{E_v}\,(D) = \mathbf{E_v}\,(D+s) \,/\, Z_{D+s \to D} \qquad \{46\}$$

Moreover, the number n_p of transverse polarization modes is reduced to $D - 1$:

$$n_p = D - 1 \qquad \{47\}$$

The energy of the directions of propagation is not lost, as the waves can propagate into a lower dimensional structure (see figure 9).

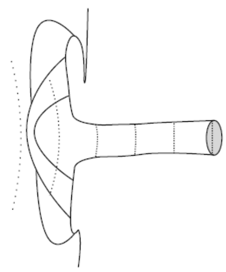

Fig.9: Propagation of waves at the ear: The three dimensional waves (loosely dotted) propagate into the effectively one dimensional auditory canal, without loss of energy.

12.9. Why is there no short-wave EZPO?

In a crystal, each atom oscillates around a fixed position in the crystal. As a consequence, each wave of coupled oscillators (each phonon) in a crystal is related to the periodic fixed positions of its atomic oscillators. As a result, there are many modes of harmonic oscillators and of phonons, and each such mode has its own ZPO and the corresponding ZPE. In contrast, the EZPOs are fully relativistic and propagating with full freedom. So there occur no such fixed points with fixed potentials, and there is no corresponding additional EZPO with a shorter wavelength and corresponding smaller EZPE than that presented in equation {46}.

Note that any ZPO that forms later can be distinguished from the EZPOs of the vacuum density.

12.10. EZPOs at D = 3

At three dimensions, the energy of a single mode is (see equations {42} and {46}):

$$\mathbf{E_v}\,(D=3) = 0.5/\,Z_{Dmax \rightarrow D=3} \qquad \{47\}$$

The length and volume of an EZPO are (see equations {43} and {45}):

$$\mathbf{L}(D=3) = Z_{Dmax \rightarrow D=3}\,;$$
$$\mathbf{V}(D=3) = Z_{Dmax \rightarrow D=3}^{3} \qquad \{48\}$$

12.11. Density of EZPOs at D = 3

The scaled density of a mode is the scaled energy divided by the scaled length. The average scaled density experienced an additional decrease by the factor $(D-1)/(D_{max}-1)$, according to the loss of transverse modes (see equation {44}). So we get:

$$<\boldsymbol{\rho}_\mathbf{v}>(D=3) = 2\cdot\mathbf{E_v}(D=3)/[\,\mathbf{V}(D=3)\cdot(D_{max}-1)]$$

We insert equations {46} and {48}. So we obtain:

$$<\boldsymbol{\rho}_\mathbf{v}>(D=3)$$
$$= 2\cdot<\boldsymbol{\rho}_\mathbf{v}>(D_{max})/[\,Z_{Dmax \rightarrow D=3}^{4}\cdot(D_{max}-1)] \quad \{49\}$$

This equation describes the density of the vacuum at the time t_f of the formation of three dimensional space. How does that density $\boldsymbol{\rho}_\mathbf{v}$ evolve after that time t_f?

12.12. EZPOs during expansion via FLE

At times after t_f, the EZPOs do not change, as there is no physical basis for a change of the EZPO, and since the invariance with respect to time is a defining criterion for the vacuum density.

As a consequence, the expansion of space is a result of an increase of the number of EZPOs. Thereby, the number of EZPOs increases according to the FLE (see Carmesin 2018a-d, Carmesin 2019 for details).

12.13. Calculation of the vacuum density

The density of the vacuum can easily be calculated. The light horizon is (see Planck 2018; Gott et al. 2005):

$$r_{lh} = 4.16\cdot10^{25}\text{ m or }\mathbf{r_{lh}} = 2.58\cdot10^{61} \qquad \{50\}$$

The space expanded (according to the FLE) from the time of D_{max} at the scaled density (of radiation) $\boldsymbol{\rho}_\mathbf{Dmax} = 0.5$ until today at the scaled density of radiation $\boldsymbol{\rho}_\mathbf{r,\,today} = 6.41\cdot10^{-127}$ (Planck 2018). Thereby the scale factor $k_{Dmax \rightarrow D=3}$ caused a decrease of the energy of radiation according to the redshift by the factor $1/k_{Dmax \rightarrow D=3}$ and an increase of the volume by the factor $(k_{Dmax \rightarrow D=3})^3$. So the density decreased by the factor $1/(k_{Dmax \rightarrow D=3})^4$. So we get the scale factor:

$$k_{Dmax \rightarrow D=3} = (\boldsymbol{\rho}_\mathbf{Dmax}/\,\boldsymbol{\rho}_\mathbf{r,\,today})^{\mathbf{1/4}} = 2.97\cdot10^{31} \quad \{51\}$$

By definition, the original length $\mathbf{L} = 1$ at D_{max} increased to the scaled light horizon $\mathbf{r_{lh}}$ by the two factors: the enlargement factor $Z_{Dmax \rightarrow D=3}$ and the scale factor $k_{Dmax \rightarrow D=3}$. So we get:

$$\mathbf{r_{lh}} = k_{Dmax \rightarrow D=3}\cdot Z_{Dmax \rightarrow D=3} \qquad \{52\}$$

We solve this equation for $Z_{Dmax \rightarrow D=3}$:

$$Z_{Dmax \rightarrow D=3} = \mathbf{r_{lh}}\,/\,k_{Dmax \rightarrow D=3} = 8.69\cdot10^{29} \quad \{53\}$$

We calculate the density of the vacuum by using equation {49} and by inserting equation {53}, and $<\boldsymbol{\rho}_\mathbf{v}> = ½$ (see equation {44}), as well as $D_{max} = 301$ (see equation {41}). So we get:

$$<\boldsymbol{\rho}_\mathbf{v}> = 5.84\cdot10^{-123} \qquad \{54\}$$

The observed scaled density of the vacuum is (Planck 2018):

$$\boldsymbol{\rho}_\mathbf{v,obs} = 4.78\cdot10^{-123} \qquad \{55\}$$

The difference between the modeled and the observed density amounts to 22 %. This accordance is already good, as that density varies by 123 orders of magnitude, and it can be improved as follows.

13. Outlook: polychromatic vacuum

In section 12 the density of the vacuum has been modeled with one EZPO and one corresponding EZPE only. However, in the course of the expansion of space, the dimensional horizon varies slightly. As a consequence the forming EZPOs vary slightly in the course of time. So the actual vacuum is a mixture of EZPOs, so it is a polychromatic vacuum. The average density of the actual polychromatic vacuum is (see Carmesin 2018a-d, Carmesin 2019):

$$<\boldsymbol{\rho}_\mathbf{v,polychromatic}> = 4.7426\cdot10^{-123} \qquad \{56\}$$

This amounts to a difference between the modeled and the observed density of 0.038 % only.

14. Outlook: dark matter

In order to see the scope of the present approach, it is mentioned here that the dark matter is obtained as a particular local minimum of the energy term $\underline{E}_{D,loc}$ (see equations {34} - {36}).

15. Experience with teaching

The students were especially interested in the topic and attended many additional meetings. They performed related observations at our school observatory (see Helmcke et al. 2018). It was possible to perform the method of problem solving in these lessons. Thereby we made transparent the goal, planned the solution in the plenum, solved it in groups and presented the results in the plenum. Hereby the microscopic part of the model including cosmic inflation was treated in 18 lessons of 90 min each, while in seven lessons we arrived at the model of the vacuum density, and in 14 lessons we modeled the dark matter. In all lessons the students actively developed their ‘process related competences’ of ‘problem solving’ and ‘modeling’ (Kultusministerium, 2017). By such problem solving, the students practice a particularly efficient method for learning (Hattie, 2009). When the students investigate the model, then they apply the essential hypothetic deductive method (Kircher, 2001; Popper 1974). Furthermore the students developed challenging ‘content related competences’ in astronomy, physics and mathematics. Some students developed projects about these topics and won prizes at Jugend forscht competitions. The students appreciated that the whole project is conceptually only based on the combination of general relativity and quantum physics, and it is numerically based on three inputs only: the three universal constants *G*, *c* and *h*. All students presented the project in public astronomy evenings in the assembly hall of our school. Thereby also a Socratic dialogue was used (see Carmesin 2018c). The assembly hall was filled with guests and many visitors discussed the topic with the students during the break.

16. Discussion

The essence of the combination of general relativity and quantum physics is worked out here: According to the uncertainty relation and to the Schwarzschild radius, there are elementary regions without observable internal structure, and on the small length scale of two such regions, we arrive at a sub curvature length scale. This is characterized by the novel equivalence principle.

In order to derive the consequences of that principle, a simple analogous structure is used here: the harmonic oscillator and coupled harmonic oscillators. With it, three fundamental results can be obtained: the era of cosmic inflation, the dark energy and the dark matter can be explained. The first two results are worked out in full detail here, so the project can directly be applied in a learning group.

The present approach provides a smooth learning process with the following features: The process is based on the two fundamental theories general relativity and quantum physics only. The process is based on three numerical inputs only: the universal constants *G*, *c* and *h*, and it arrives at a precise accordance with observations. The analogy based learning process proposed here has three mile stones, the equivalence principle, the harmonic oscillator and its transfer to the energy term $\underline{E}_{D,loc}$ (see eq. {36}), as well as coupled harmonic oscillators and the transfer to the vacuum density or dark energy. Thereby, the two analogies integrate the new knowledge into existing knowledge, and correspondingly, a very high learning efficiency is achieved (see Hattie 2009).

17. Literature

Ballentine, Leslie (1998): Quantum Mechanics. London and Singapore: World Scientific Publishing.

Bronstein, Matvei, P. (1936): Quantentheorie schwacher Gravitationsfelder. Phys. Z. Sowjetunion, 9, pp. 140-157.

Broy, Benedict Johannes (2016): Inflation and effective Shift Symmetries. Hamburg: University Hamburg. Thesis.

Bures, Martin (2011): Quantum Physics with Extra Dimensions. Brno: Masaryk University, Thesis.

Carmesin, Hans-Otto and Carmesin, Ellen (2014): How Old is the Universe? PhyDid B, ISSN 2191-379X.

Carmesin, Hans-Otto (2017): Vom Big Bang bis heute mit Gravitation – Model for the Dynamics of Space. Berlin: Verlag Dr. Köster.

Carmesin, Hans-Otto (May 2018a): Entstehung dunkler Materie durch Gravitation - Model for the Dynamics of Space and the Emergence of Dark Matter. Berlin: Verlag Dr. Köster.

Carmesin, Hans-Otto (July 2018b): Entstehung dunkler Energie durch Quantengravitation - Universal Model for the Dynamics of Space, Dark Matter and Dark Energy. Berlin: Verlag Dr. Köster.

Carmesin, Hans-Otto (November 2018c): Entstehung der Raumzeit durch Quantengravitation – Theory for the Emergence of Space, Dark Matter, Dark Energy and Space-Time. Berlin: Verlag Dr. Köster.

Carmesin, Hans-Otto (2018d): A Model for the Dynamics of Space - Expedition to the Early Universe. PhyDid B Internet Journal, pp. = 1-9.

Carmesin, Hans-Otto (July 2019): Die Grundschwingungen des Universums - The Cosmic Unification. Berlin: Verlag Dr. Köster.

Einstein, Albert (1915): Die Feldgleichungen der Gravitation. Sitzungsberichte der Preuss. Akademie der Wissenschaften, pp. 844-847.

Einstein, Albert (1917): Kosmologische Betrachtungen zur allgemeinen Relativitätstheorie. Sitzungsberichte der Preuss. Akademie der Wissenschaften, pp. 142-152.

Fornasini, P.; Grisenti, R. (2015): On EXAFS Debye - Waller factor and recent advances. Journal of Sychrotron Radiation, 22, pp. 1242-1257.

Friedmann, Alexander (1922): Über die Krümmung des Raumes. Z. f. Physik, 10, 377-386.

Gauss, Carl Friedrich (1813): Theoria attractionis corporum sphaeroidicorum ellipticorum homogeneorum – methoda novo tractata. Societ. Reg. Scient. Tradita. 1-24.

Gott, Richard J.; Juric, Mario; Schlegel, David; Hoyle, Fiona; Vogeley, Michael; Tegmark, Max; Bahcal, Neta and Brinkmann, Jon (2005): A Map of the Universe. The Astrophysical Journal, 624, pp. 463-484.

Guth, Alan (1981): Inflationary Universe: A possible to the horizon and flatness problem. Phys. Rev. D 23, 347-356.

Hattie, John (2009): Visible Learning. London: Routledge.

Heid, R.; Bohnen, K.-P. and Reichardt, W. (1999): Ab initio phonon spectra from a supercell approach. Physica B, 263, pp. 432-435.

Heisenberg, Werner (1927: Über den anschaulichen Inhalt der quantentheoretischen Kinematik und Mechanik. Z. f. Phys., 43, pp. 172-198.

Helmcke, Ben Joshua; Carmesin, Hans-Otto; Sprenger, Lennert und Brüning, Paul (2018): Three methods for the observation of the Big Bang with our school telescope. PhyDid B.

Hoskin, Michael (1997): The Cambridge Concise History of Astronomy. Cambridge: Cambridge University Press.

Kircher, Ernst and Girwidz, Raimund and Häußler, Peter (2001): Physikdidaktik. Berlin: Springer. 2. Auflage.

Kultusministerium, Niedersächsisches (2017): Kerncurriculum für das Gymnasium - gymnasiale Oberstufe, die Gesamtschule - gymnasiale Oberstufe, das Fachgymnasium, das Abendgymnasium, das Kolleg, Chemie, Niedersachsen. Hannover: Niedersächsisches Kultusministerium.

Lee, John M. (1997): Riemannian Manifolds: An Introduction to Curvature. New York: Springer Verlag.

Lemaitre, Georges (1927): Un Univers homogene de masse constante et de rayon croissant rendant compte de la vitesse radiale des nebuleuses extra-galactiques. Annales de la Societe Scientifique de Bruxelles. A47, 49-59.

Lohse, Michael et al. (2018): Exploring 4D Quantum Hall Physics with a 2D Topological Charge Pump. Nature, 553, pp. 55-58.

Michell, John (1784): On the means of discovering the distance, magnitude, etc. of the fixed stars in consequence of the diminution of the velocity of their light, in case such a diminution should be found to take place in any of them, and such other data should be procured from observations, as would be farther necessary for that purpose. Phil. Trans. R. Soc. Lond., 74, pp. 35-57.

Perlmutter, S. et al. (1998): Discovery of a Supernova Explosion at Half the Age of the Universe. Nature, 391, pp. 51-54.

Planck, Max (1899): Über irreversible Strahlungsvorgänge. Sitzungsberichte der Königlich Preußischen Akademie der Wissenschaften zu Berlin. Berlin: Verlag der Kgl. Preuß. Akad. der Wiss., 440-480.

Planck Collaboration (2018): Planck 2018 Results: Cosmological Parameters. Astronomy and Astrophysics, pp. 1-71.

Popper, Karl (1974): Objektive Erkenntnis. 2. Auflage. Hamburg: Hoffmann und Campe.

Riess, Adam G. et al. (2000): Tests of the Accelerating Universe with Near-Infrared Observations of a High-Redshift Type Ia Supernova. The Astrophysical Journal, 536, pp. 62-67.

Schwarzschild, Karl (1916): Über das Gravitationsfeld eines Massenpunktes nach der Einstein'schen Theorie. Sitzungsberichte der Deutschen Akademie der Wissenschaften, pp. 186-196.

Schrödinger, Erwin (1926): Quantisierung als Eigenwertptoblem I. Annalen der Physik, 79, pp. 361-376.

Smoot, George F. (2007): Nobel Lecture: Cosmic microwave background radiation anisotropies: Their discovery and utilization. Review of Modern Physics, 79, pp. 1347-1379.

Sprenger, Lennert und Carmesin, Hans-Otto (2018): A Computer Simulation of Cosmic Inflation. PhyDid B.

Zilberberg, Oded et al. (2018): Photonic topological pumping through the edges of a dynamical four-dimensional quantum Hall system. Nature, 553, pp. 59-63.

Zwicky, Fritz (1933): Die Rotverschiebung von extragalaktischen Nebeln. Helvetica Physica Acta, 6, pp. 110-127.

Acknowledement

I am grateful to Matthias Carmesin for many helpful discussions. I thank my students Paul Brüuning, Lennert Sprenger, Ben Joshua Helmcke and Ole Rademacker for interesting discussions. I am very grateful to I. Carmesin for many helpful discussions.